Proceedings of the International Conference on Industrial Engineering and Operations Management

Publisher: IEOM Society International, USA DOI: 10.46254/EU08.20250222
Published: July 2, 2025

Sensitivity Analysis of a Metal Hydride Reactor Utilizing $LaNi_{4.9}Sn_{0.1}$ Metal Hydride

Douw G Faurie, Kasturie Premlall and Andrei Kolesnikov
Department of Chemical Metallurgical and Materials Engineering
Tshwane University of Technology
Pretoria, Republic of South Africa
GerbrandFaurie@gmail.com, PremlallK@tut.ac.za, KolesnikovA@tut.ac.za

Mykhaylo Lototskyy
HySA Systems, South African Institute for Advanced Materials Chemistry
University of the Western Cape
Cape Town, Republic of South Africa
MLototskyy@uwc.ac.za

Abstract

Solid-state hydrogen storage in the form of a metal hydride has emerged as a safe and low-pressure storage solution with a competitive volumetric energy density. In this technology, hydrogen is stored in a hydride-forming metal, specifically, $LaNi_{4.9}Sn_{0.1}$ metal hydride in this study, through exothermic absorption, which can then be discharged through endothermic desorption. This results in a complex system where the rate of sorption is dependent on external factors as well as internal factors, making control of the unit difficult. This study focuses on the sensitivity analysis of a metal hydride reactor to deepen the understanding of the unit's operation outside of normal operation conditions. This was done using an experimentally validated computational fluid dynamics model, which reduces risks to the unit and costs of taking the unit out of circulation to conduct this study. The simulation model performed to satisfactory levels with an R-squared of greater than 0.9 and minimal mean squared error. The sensitivity analysis showed that during hydrogen charging, there is a slowing effect experienced at higher cooling fluid temperatures with an accelerating effect at higher feed gas pressures. The sensitivity analysis showed a similar relationship, just inverse, was observed during hydrogen discharging, with the required gas pressure slowing the rate of hydrogen flow and higher heating fluid temperatures accelerating the hydrogen flow rate. Finally, the sensitivity analysis showed that there is a certain innate thermodynamic limit beyond which the operation slows to a crawl or stops completely.

Keywords
Metal Hydride Reactors, Computational Fluid Dynamics, Sensitivity Analysis, Solid-Phase Hydrogen Storage, Hydrogen Energy.

1. Introduction

1.1 Background and Justification

The world's energy demand is increasing, and with the looming threat of climate change, high oil prices and the inevitable depletion of fossil fuels, the world is in dire need of alternative energy solutions. The effect is that renewable energy research has gotten momentum, among these possible replacements for conventional petroleum-based fuel (Abdechafik et al., 2024). Hydrogen is an abundant and clean energy carrier with the highest energy density (Li et al.,

2024), in terms of mass, for all known non-nuclear fuels. Hydrogen storage can either be in gas form, liquid form or employing chemical-physical methods (Yartys & Lototsky, 2004; Abdechafik et al., 2024).

The United States of America's Department of Energy has made available sixty-four million dollars in funding for eighteen projects to advance the Hydrogen at Scale (H2@Scale) concept. H2@Scale is an endeavour to test the potential of the hydrogen economy at a macro scale. Figure 1 below illustrates the conceptual framework in which H2@Scale would be integrated into the existing infrastructure (Hydrogen and Fuel Cell Technologies Office, 2020).

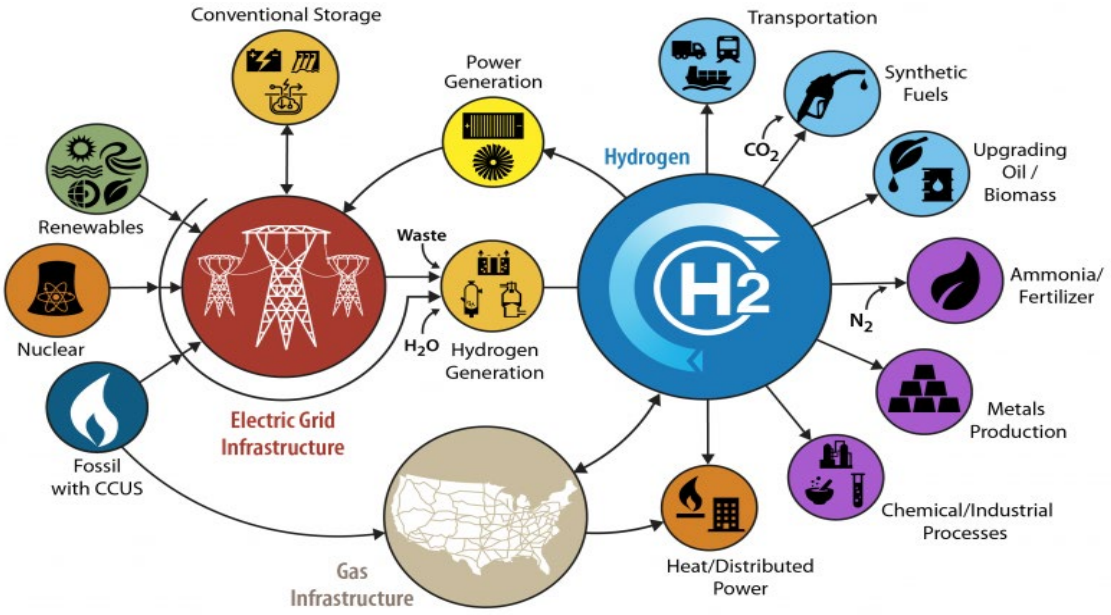

Figure 1. United States of America's H2@Scale concept (Hydrogen and Fuel Cell Technologies Office, 2020)

Excess energy would be used to generate hydrogen for numerous industrial uses such as fuels, fertilisers, chemical products and power storage. Power storage through hydrogen would be used in tandem with conventional energy storage methods as well as lower the dependency on natural gas for heating. Key aspects of the framework are denoted in the plan to use the existing nationwide gas infrastructure to transport the hydrogen to each destination for use (Hydrogen and Fuel Cell Technologies Office, 2020; Handique et al., 2024; Jeje et al., 2024).

The main challenge facing hydrogen energy is the effective storage of hydrogen, with the main goal of hydrogen storage innovation being to achieve lightweight and compact solutions to satisfy mobile storage needs (Prachi et al. 2016; Qureshi et al., 2024).

Hydrogen can be stored using conventional methods, such as cryogenic liquefaction and gas compression, or using physical-chemical methods (Yartys & Lototsky, 2004; Prachi et al. 2016; Drawer et al. 2024). Conventional methods are characterised as physical processes where the hydrogen does not undergo chemical interactions, whereas physical-chemical methods involve some form of chemical change (Yartys & Lototsky, 2004; Drawer et al. 2024). Furthermore, conventional hydrogen storage tends to be bulky and heavy, while physical-chemical hydrogen storage is lighter and more compact (Prachi et al. 2016; Drawer et al. 2024).

Gas-state hydrogen storage, otherwise known as compression-based hydrogen storage, is housed in gas cylinders, underground cavities like cave systems or mines and inside storage pipelines. Bulk storage of hydrogen in the gas state requires high pressures, which can pose safety risks and necessitate heavy tanks, significantly reducing the gravimetric energy density of the hydrogen storage (Churchard et al., 2011; Prachi et al. 2016; Li et al., 2022; Abdechafik et al., 2024; Drawer et al. 2024).

Liquid-state hydrogen storage comes in two forms: cryogenic-based hydrogen storage and physical-chemical-based storage. Conventional storage refers to cryogenic storage tanks where the hydrogen is cooled into a liquid state and stored under low temperatures to maintain that state (Churchard et al., 2011; Prachi et al. 2016; Abdechafik et al., 2024; Drawer et al. 2024).

In contrast, physical-chemical storage involves the reaction of hydrogen into a liquid phase, resulting in the formation of liquid hydrides and combustible chemicals, such as methanol and ammonia (Churchard et al., 2011; Prachi et al. 2016).

Hydrogen cryogenic liquefaction, however, is a highly energy-exhaustive process. Furthermore, long-term storage losses may be significant, as hydrogen may boil off or require continuous refrigeration and compression maintenance (Churchard et al., 2011; Prachi et al. 2016; Drawer et al. 2024).

Solid-state hydrogen storage involves bulk sorption into metals to form metal hydrides. Hydrogen can then be recovered from metal hydrides using thermal stimulation. Moreover, solid hydrogen storage addresses the challenges faced by physical liquid and gas state storage solutions (Ghritalahre et al., 2023). Besides metal hydride forming metals zeolites, metal-organic-frameworks, and carbon nanotubes can also undergo sorption of hydrogen (Yartys & Lototsky, 2004; Churchard et al., 2011; Prachi et al. 2016; Abdechafik et al., 2024; Drawer et al. 2024).

Solid-state hydrogen storage, specifically hydride-forming metal solid-state hydrogen storage, has emerged as a possible solution to the storage challenges (Prachiet al. 2016; Busqué et al., 2017; Dong et al., 2022; Salman et al., 2022; Cavo et al., 2023). Hydrogen energy systems have decoupled power and energy features, allowing for cost-effective expansion and large-scale hydrogen-based energy storage, which is more economical than alternatives. However, high-pressure hydrogen storage results in a higher amount of maintenance, repair and expert operators (Bellosta von Colbe et al., 2019).

This makes these storage solutions unideal for off-grid applications and hydride-based storage solutions superior to off-grid applications (Bellosta von Colbe et al., 2019). A 5 kW hydrogen fuel cell metal hydride system can be fully recharged in around 20 min (Song et al., 2014; Lototskyy et al., 2017). Furthermore, hydrides also act as compressors for hydrogen without the need for mechanical systems to achieve the desired pressures (Lototskyy et al., 2018; Tarasov et al., 2020).

Hydrogen storage densities of the three hydrogen storage states are vastly different in comparison. It should be noted that at room temperature and 10 megapascals, gas state hydrogen reaches approximately 7.5 g/L. In contrast, liquid-state hydrogen achieves approximately 30 g/L at 30 megapascals and nearly 50 g/L at 100 megapascals (Aziz, 2021). However, most hydrides exceed 40 g/L hydrogen capacity, with some hydrides exceeding 100 g/L hydrogen capacity at maximum capacity while struggling with gravimetric capacity (Pasini et al., 2013).

1.2 Aim and Objectives

This study aimed to perform a sensitivity analysis of a metal hydride reactor. This was done by formulating a metal hydride reactor model in a computational fluid dynamics simulation environment. This model was then validated using experimental data to show that the model represents, to a satisfactory degree, what could be experienced experimentally. Finally, this model is then used to perform a sensitivity analysis regarding the feed gas pressure and cooling fluid temperature for charging. While discharging the required gas pressure and the heating fluid temperature were then considered.

2. Literature Review

In selecting a non-ideal gas-metal isotherm model, the model published by Lototskyy (2016) is semi-empirical. It allows the model to capture accurate isotherms where multiple plateaus regarding pressures occur in more complex hydride-forming metal alloys.

The non-ideal gas-metal isotherm model published by Lototskyy (2016) was adapted to be used in this study. The model is semi-empirical and calculates the concentration (C) of hydrogen inside the lattice as a function of pressure (P) and temperature (T). The total model consists of forty-five Equations, some of which require numerical differentiation and integration to solve.

Figure 2 shows a flow chart of the logical progression of the model. This progression has been divided into ten analytical steps with Pressure and Temperature along with Pressure-Concentration-Temperature (PCT) Parameters as the inputs and the output as Concentration (Faurie & Premlall, 2025).

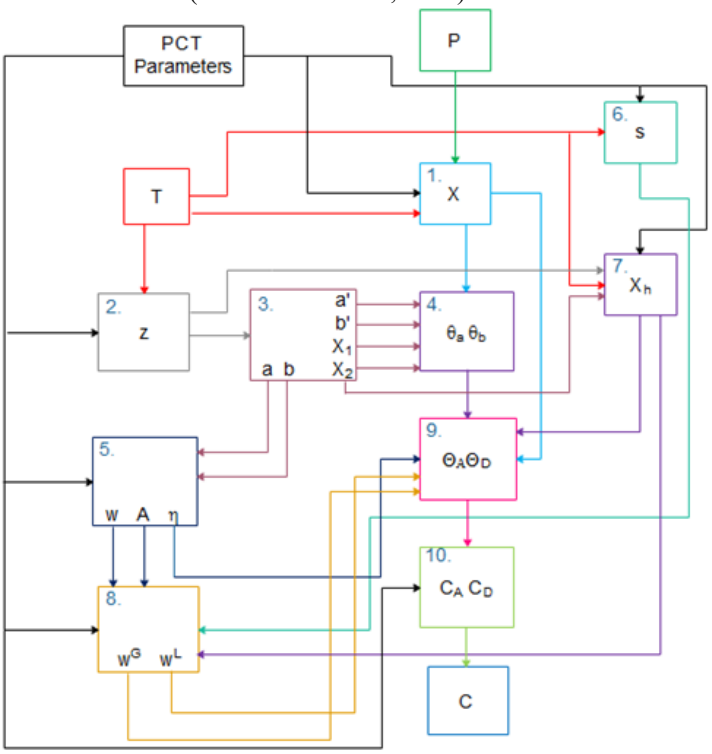

Figure 2. Flow chart showing steps adapted model used to calculate metal hydride Isotherm (Faurie & Premlall, 2025).

Figure 3 shows the simulation performance in calculating the pressure-concentration-temperature isotherms for the three different types of AB5 hydride-forming metal. Here, pressure is in atmospheres (atm), and concentration is in normal litres per kilogram (NL/kg) (Faurie & Premlall, 2025).

In Figure 3, each colour represents a different temperature and, by extension, a different pressure-concentration isotherm. Moreover, the solid markers and solid line represent absorption experimental data and the absorption simulation, respectively. The hollow markers and dashed lines represent the desorption experimental data and the desorption simulation, respectively (Faurie & Premlall, 2025).

The model prediction closely follows the experimental data overall. It does this regardless of the different temperatures and the hydride-forming metal's several plateaus. This holds for both the absorption and desorption isotherms. The only exception is on the 294 K absorption isotherm the model deviates significantly from the experimental data.
This error occurs as the model divides isotherms into segments to account for isotherms having multiple plateau phenomena regarding logarithmic pressure. Thus, during fitting, a secondary plateau was incorrectly placed on the 294 K. However, this still resulted in the best fit currently and was, as such, still used in the simulation of the isotherms represented in Figure 3 (Faurie & Premlall, 2025).

The model prediction closely follows the experimental data overall. It does this regardless of the different temperatures and the hydride-forming metal's several plateaus. This holds for both the absorption and desorption isotherms. This resulted in the best fit currently and was, as such, still used in the simulation of the isotherms represented in Figure 3 (Faurie & Premlall, 2025). Regarding the error analysis performed, a very low two-dimensional error fell below 0.15 absolute two-dimensional error (Faurie & Premlall, 2025).

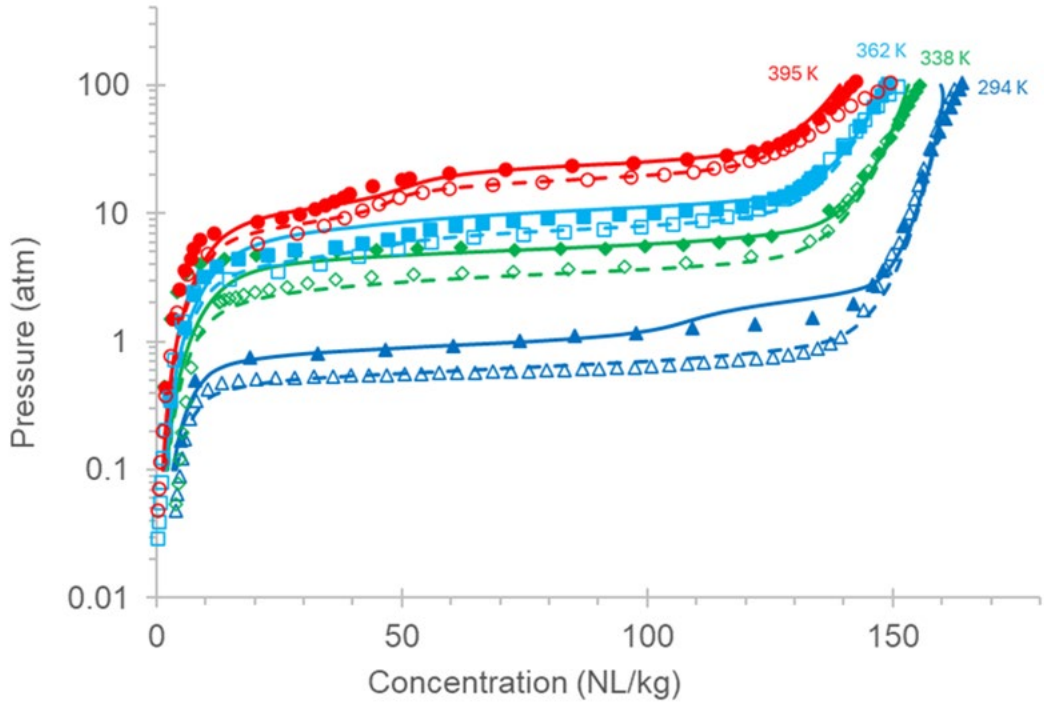

Figure 3. $LaNi_{4.9}Sn_{0.1}$ Isotherm simulation. Solid and hollow markers represent experimental absorption and desorption data, respectively. Similarly, solid lines and dashed lines represent simulated absorption and desorption data. Each isotherm pair is labelled with the temperature (Faurie & Premlall, 2025).

Table 1 represents the isotherm fitting parameters for the specific $LaNi_{4.89}n_{0.1}$ hydride-forming metal alloy (Lototskyy, 2016; Faurie & Premlall, 2025).

Table 1. PCT Isotherm fitting parameters (Lototskyy, 2016; Faurie & Premlall, 2025)

Parameter	$LaNi_{4.9}Sn_{0.1}$	
	Segment 1	Segment 2
C_{max}	0.188	
W	0.29	0.71
T_C (K)	471	465
ΔS^0 (J/mol-H_2-K)	-74.5	-108.0
ΔH^0 (J/mol-H_2)	-22907	-33008
ΔG_h(J/mol-H_2)	2373	1079
w_0^A	0.199	0.137
η_0^A	0.59	0.69
A_0^A	2.164	0.005
s_0^A	0.88	0.90
w_0^D	0.195	0.140
η_0^D	0.61	0.43
A_0^D	1.142	0.108
s_0^D	0.88	0.90
m	0.097	0.209
T_0 (K)	396	461
ρ_{SH}	0.5616	0.6502

Considering the modelling of metal hydride reactors, the rate of sorption of a metal hydride is described by Baldissin and Lombardo, (2009) as the following:

$$\dot{m} = C_A exp\left(-\frac{E_A}{RT}\right) \ln\left(\frac{P_g}{P_{eq}}\right)(\rho_{ss} - \rho_s) \text{ (1)}$$

$$\dot{m} = C_D exp\left(-\frac{E_D}{RT}\right) \frac{P_g - P_{eq}}{P_{eq}} (\rho_s - \rho_0) \text{ (2)}$$

Here, Equation 1 is relevant for absorption and Equation 2 is relevant for desorption. This is derived from the unsteady state relationship between the bed density and sorption rate described by Akanji et al., (2010) and Jemni et al., (1999):

$$(1 - \varepsilon)\frac{\partial \rho}{\partial t} = \dot{m} \text{ (3)}$$

Here:

$\dot{m}$	-	Hydrogen sorption rate in mass/volume/time	ρ_0	-	Standard hydride density
ρ_s	-	Dynamic hydride density	ρ_{ss}	-	Final saturated hydride density
C_A	-	Absorption rate constant	C_D	-	Desorption rate constant
E_A	-	Absorption activation energy	E_D	-	Desorption activation energy
P_g	-	The pressure of the gas in the tank	P_{eq}	-	The pressure of the gas in the hydride
T	-	Temperature	R	-	Ideal gas constant
ε	-	Porosity	t	-	Time
∂	-	Partial differential	ρ	-	Hydride density

Here dynamic hydride density is defined as:

$$\rho_s = \frac{\partial \rho}{\partial t} \text{ (4)}$$

The Concentration (C) of hydrogen in the metal hydride is described by Lototskyy (2016) as:

$$C = \frac{H}{M} \text{ (5)}$$

Here:

C	-	Concentration	H	-	Moles of hydrogen
M	-	Moles of metal hydride			

Which can be used as a governing Equation and expanded to the following:

$$C_s = \left(\frac{H}{M}\right)_s \text{ (6)}$$

$$C_{ss} = \left(\frac{H}{M}\right)_{ss} \text{ (7)}$$

Here:

C_s	-	Dynamic hydride concentration	C_{ss}	-	Final Saturated hydride concentration
$\left(\frac{H}{M}\right)_s$	-	Saturated molar hydrogen to metal ratio	$\left(\frac{H}{M}\right)_{ss}$	-	Final Saturated molar hydrogen to metal ratio

Based on the model used by Mellouli et al., (2009), Equations 8 and 9 can be defined using a concentration in place of density as expressed by:

$$\dot{m} = C_A exp\left(-\frac{E_A}{RT}\right) \ln\left(\frac{P_g}{P_{eq}}\right)\left(\frac{\rho_s M_g}{M_s}\right)(C_{ss} - C_s) \text{ (8)}$$

$$\dot{m} = C_D exp\left(-\frac{E_D}{RT}\right)\left(\frac{P_g - P_{eq}}{P_{eq}}\right)\left(\frac{\rho_s M_g}{M_s}\right)(C_s) \text{ (9)}$$

Here:

M_s	-	Molar weight of solid hydride	M_g	-	Molar weight of hydrogen

Table 2 represents the sorption model used for the computational fluid dynamics simulation.

Table 2. Sorption model parameters

Parameter	Symbol	Value
Initial hydride density	ρ_0	8400 kg m^{-3} (Walker, 2008)
Hydride molecular weight	M_s	432 kg $kmol^{-1}$ (Calculated from composition)
Hydrogen molecular weight	M_g	2 kg $kmol^{-1}$ (Baldissin & Lombardo, 2009)
Hydride specific heat	C_{ps}	356 J kg^{-1} K^{-1} (Dehouche, et al. 2005)
Hydrogen specific heat	C_{pg}	14890 J kg^{-1} K^{-1} (Baldissin & Lombardo, 2009)
Reaction enthalpy	ΔH^0	-40000 J mol^{-1} (Fitted)
Reaction entropy	ΔS^0	-110 J kg^{-1} K^{-1} (Fitted)
Absorption kinetic constant	C_A	1 s^{-1} (Fitted)
Absorption activation energy	E_A	19000 J mol^{-1} (Fitted)
Desorption kinetic constant	C_D	3.5 s^{-1} (Fitted)
Desorption activation energy	E_D	25000 J mol^{-1} (Fitted)

The flow of the hydrogen gas can be simplified to Darcy's Law to account for the pressure drop over the porous bed represented by Equations 3.48 and 3.49 (Wang et al., 2019).

$$\frac{\partial}{\partial t}(\varepsilon_p \rho) + \nabla(\rho u) = Q_m \quad (10)$$

$$u = -\frac{K}{\mu}\nabla p \quad (11)$$

Likewise, the flow of heat in the porous bed can be simplified to a porous heat conduction law which combines convective and conductive heat transfer represented by Equations 3.50 and 3.51 (Wang et al., 2019).

$$(\rho C_p)_{eff}\frac{\partial}{\partial t} + \rho C_p u \cdot \nabla T + \nabla q = Q + Q_{vd} \quad (12)$$

$$q = -k_{eff}\nabla T \quad (13)$$

3. Methods

Figure 5 shows the experimental setup of the metal hydride reactor, which consists of a single internal and single shell pass system as a hybrid of the conventional designs filled with $LaNi_{4.9}Sn_{0.1}$ hydride-forming metal. As a digital representation of the setup used by Lototskyy et al. (2018) as seen in Figure 5, Figure 4 illustrates the simulation environment geometry, which is a simulation-based likeness under the assumptions of the study. The mesh for the simulation had 581 vertices with 1415 elements, with an average mesh quality of 0.6428.

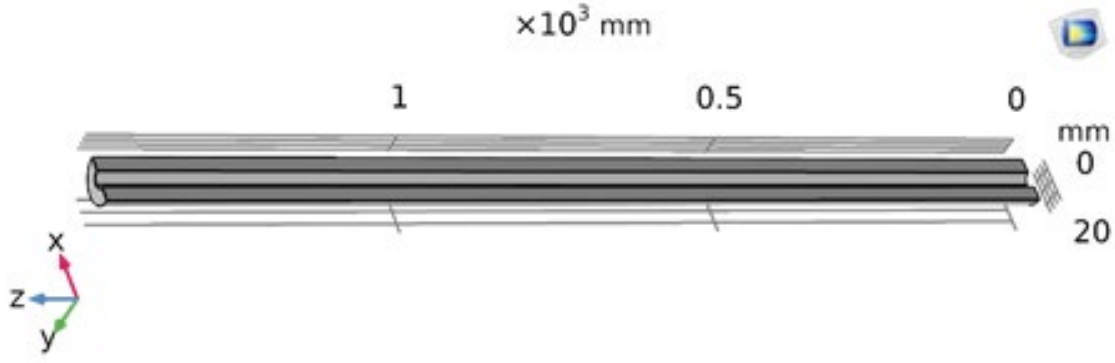

Figure 4. Hydride-based hydrogen compressor simulation environment cross-sectioned geometry

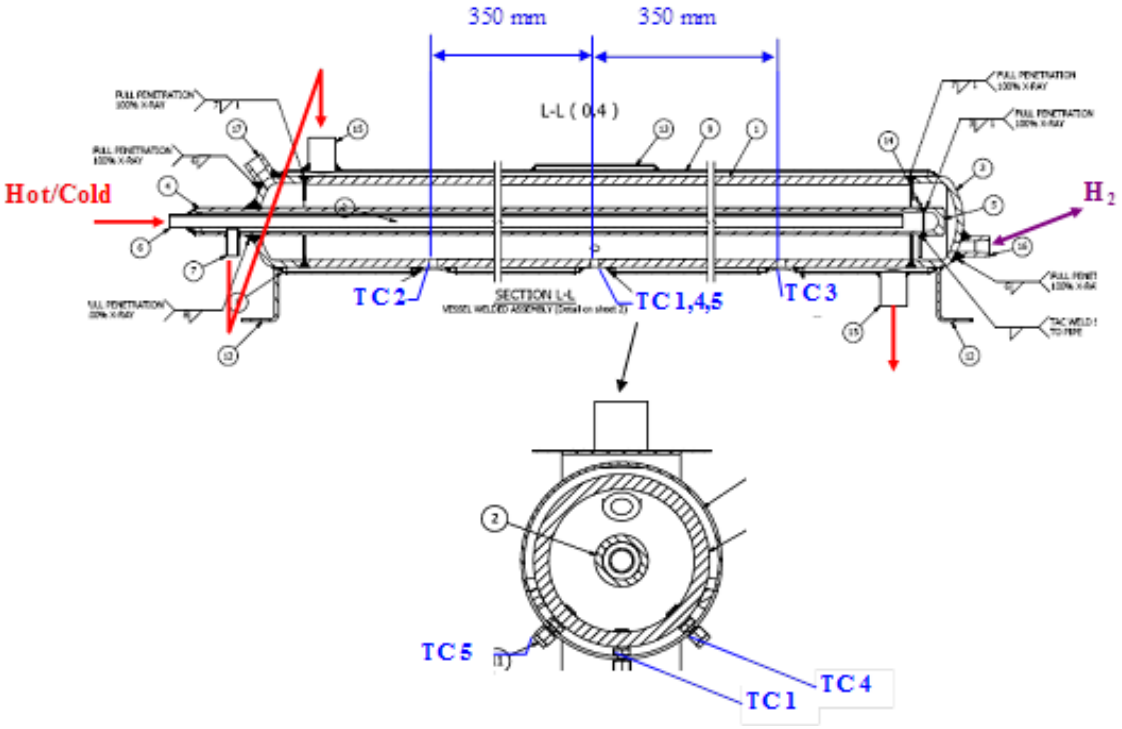

Figure 5. Schematic diagram of hydride-based hydrogen compressor (Lototskyy et al. 2018)

4. Data Collection

The computational fluid dynamics model and neural network performance were determined by the R-squared statistic of the simulated data against the experimental data, represented by Equation 15, and the mean squared error, represented by Equation 14.

$$S^2 = \frac{1}{n}\sum_{i=1}^{n}\left(Y_i - \hat{Y}_i\right)^2 \quad (14)$$

$$R^2 = \frac{\sum_{i=1}^{n}(\hat{Y}_i - \bar{Y})^2}{\sum_{i=1}^{n}(Y_i - \bar{Y})^2} \quad (15)$$

Here:

s^2	-	Mean squared error	R^2	-	R-squared
i	-	Observation number	n	-	Number of data points
$\hat{Y}_i$	-	Predicted value	Y_i	-	Observed Value
$\bar{Y}$	-	Observed mean value			

Validation data were obtained at normal operational conditions, for charging, water at 15 °C to 20 °C and a feed gas pressure around 5 bar were used. On the other hand, for discharging, the desired gas pressure delivered by the unit was set at around 16 bar on the regulator, and to achieve that, steam of 135 °C to 145 °C was used.

5. Results and Discussion

5.1 Simulation Validation

Figure 6 demonstrates graphically the accuracy of the computational fluid dynamics model during charging against two experimental validation runs. Specifically, in Figure 6A, the hydrogen feed gas pressure was at 5.5 bar with cooling fluid at 15 °C and in Figure 6B, the hydrogen feed gas pressure was at 4.9 bar with cooling fluid at 18 °C. In Figures 3.5 and 3.6, the abbreviation “sim” is used for the computational fluid dynamics simulation and experimental, and “exp” is used.

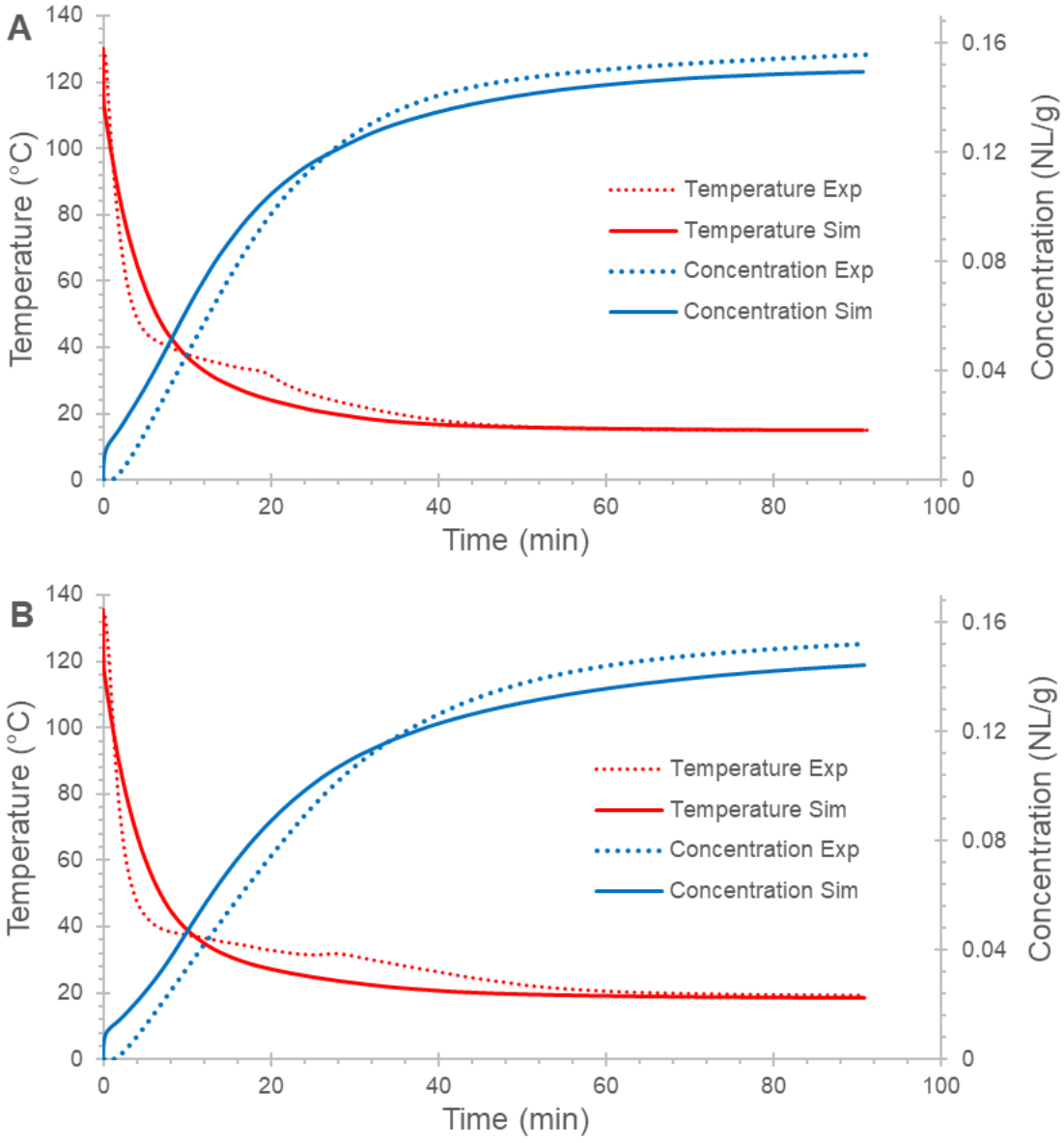

Figure 6. Absorption computational fluid dynamics model validation with time versus concentration and temperature with (A) feed gas pressure at 5.5 bar with cooling fluid at 15 °C and (B) feed gas pressure at 4.9 bar with cooling fluid at 18 °C

Figure 7 demonstrates graphically the accuracy of the computational fluid dynamics model during discharge against two experimental validation runs. Specifically, in Figure 7A the hydrogen discharge gas pressure was at 16.4 bar with heating fluid at 135 °C and in Figure 7B the hydrogen discharge gas pressure was at 16 bar with heating fluid at 142 °C.

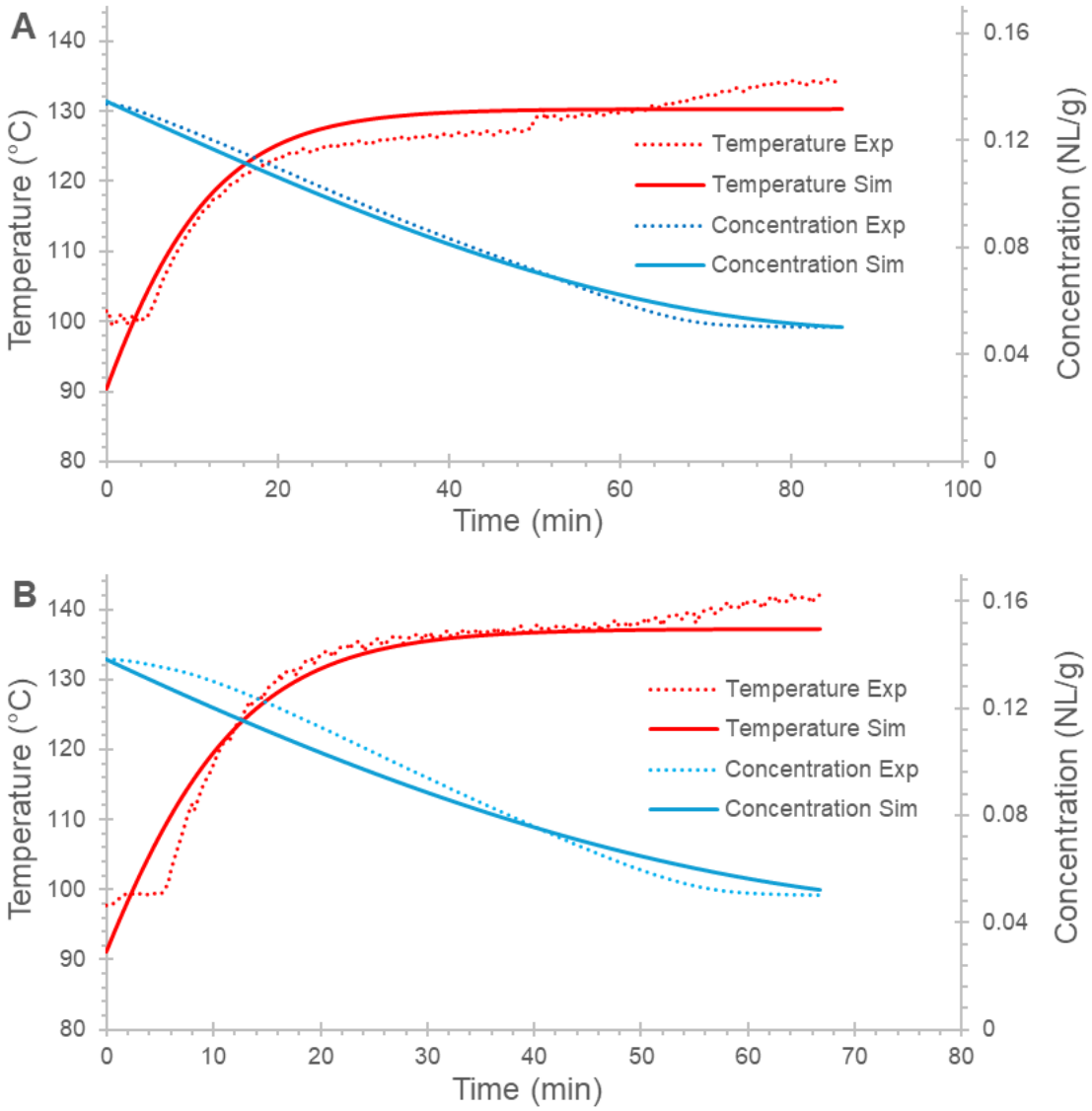

Figure 7. Desorption computational fluid dynamics model validation with time versus concentration and temperature with (A) discharge gas pressure at 16.4 bar with heating fluid at 135 °C and (B) discharge gas pressure at 16 bar with heating fluid at 142 °C

Regarding Figure 6A and Figure 6B, both have the same general trend when comparing the experimental with the simulated data, with the simulation overshooting for about 40 min and then undershooting passed that point. Similarly, regarding Figure 7A and Figure 7B, both have the same general trend when comparing the experimental with the simulated data, with overshooting and undershooting on the part of the simulation.

Table 3 represents the summarised validation of the computational fluid dynamics simulation against two charges and two discharge experimental trials. With R-squared close to 1 and low mean squared errors, the model performed well, with the 4.9 bar 18 °C trial showing a lower-than-desired bed temperature accuracy.

Table 3. Computational fluid dynamics model performance as measured against experimental validation trials

Absorption					
Feed gas pressure	Heating fluid temperature	Concentration R^2	Concentration S^2	Bed temperature R^2	Bed temperature S^2
5.5 bar	15 °C	0.9490	1.01E-4	0.9418	14.59
4.9 bar	18 °C	0.9240	1.62E-4	0.8598	31.31
Desorption					
Discharge gas pressure	Heating fluid temperature	Concentration R^2	Concentration S^2	Bed temperature R^2	Bed temperature S^2
16.4 bar	135 °C	0.9905	7.31E-06	0.9051	7.48
16 bar	142 °C	0.9510	4.41E-05	0.9443	7.19

5.2 Sensitivity Analysis Results

Figure 8 illustrates the system sensitivity to feed gas pressure and cooling fluid temperature during hydrogen absorption, or charging state, generated by the computational fluid dynamics simulation. Specifically, Figure 8A shows the charge as a percentage after 90 minutes of hydrogen absorption. This is the fraction of the equilibrium absorption concentration achieved in 90 minutes.

Similarly, Figure 8B shows the equilibrium absorption concentration, thus the highest concentration achievable. These are represented in terms of feed gas pressure and cooling fluid temperature. This equilibrium absorption concentration was calculated using the isotherm model represented in Figure 3 and would otherwise be the maximum concentration achievable at the respective pressure and temperature.

Regarding Figure 8A, at lower cooling fluid temperatures, feed gas pressure seems to have a significant effect. However, feed gas pressure at higher cooling fluid temperatures seems to have a much greater effect. Additionally, at higher feed gas pressures, the cooling fluid seems to have a reduced effect when compared to the effect it has at lower feed gas pressures.

As such, when considering Figure 8A, higher feed gas pressures aid in speeding up the charging process, while higher cooling fluid temperatures slow down the charging process. However, the relationship is further complicated by higher feed gas pressures counteracting the slowing effect of higher cooling fluid temperatures. Moreover, lower cooling fluid temperatures aid in the absorption rate by cooling the bed, lowering the need for higher feed gas pressures.

This is exactly what is hypothesised when considering Equation 8 and the isotherms represented in Figure 3. More so when considering Figure 8B, which has a very similar trend to Figure 8A, suggesting a relationship between the equilibrium absorption concentration and the charge amount, as well as the charge rate.

Figure 9 illustrates the system sensitivity to required discharge gas pressure and heating fluid temperature during hydrogen desorption, or discharging state, generated by the computational fluid dynamics simulation. Specifically, Figure 9A shows the discharge as a percentage after 80 minutes of hydrogen desorption. This is the fraction of the total available hydrogen concentration discharged in 80 minutes. 80 minutes would be the full load discharge at the maximum rate it can be at the required pressure.

Similarly, Figure 9B shows the equilibrium desorption concentration, thus the lowest concentration achievable. These are represented in terms of required discharge pressure and heating fluid temperature. This equilibrium desorption concentration was calculated using the isotherm model represented in Figure 3 and would otherwise be the lowest concentration achievable at the respective pressure and temperature.

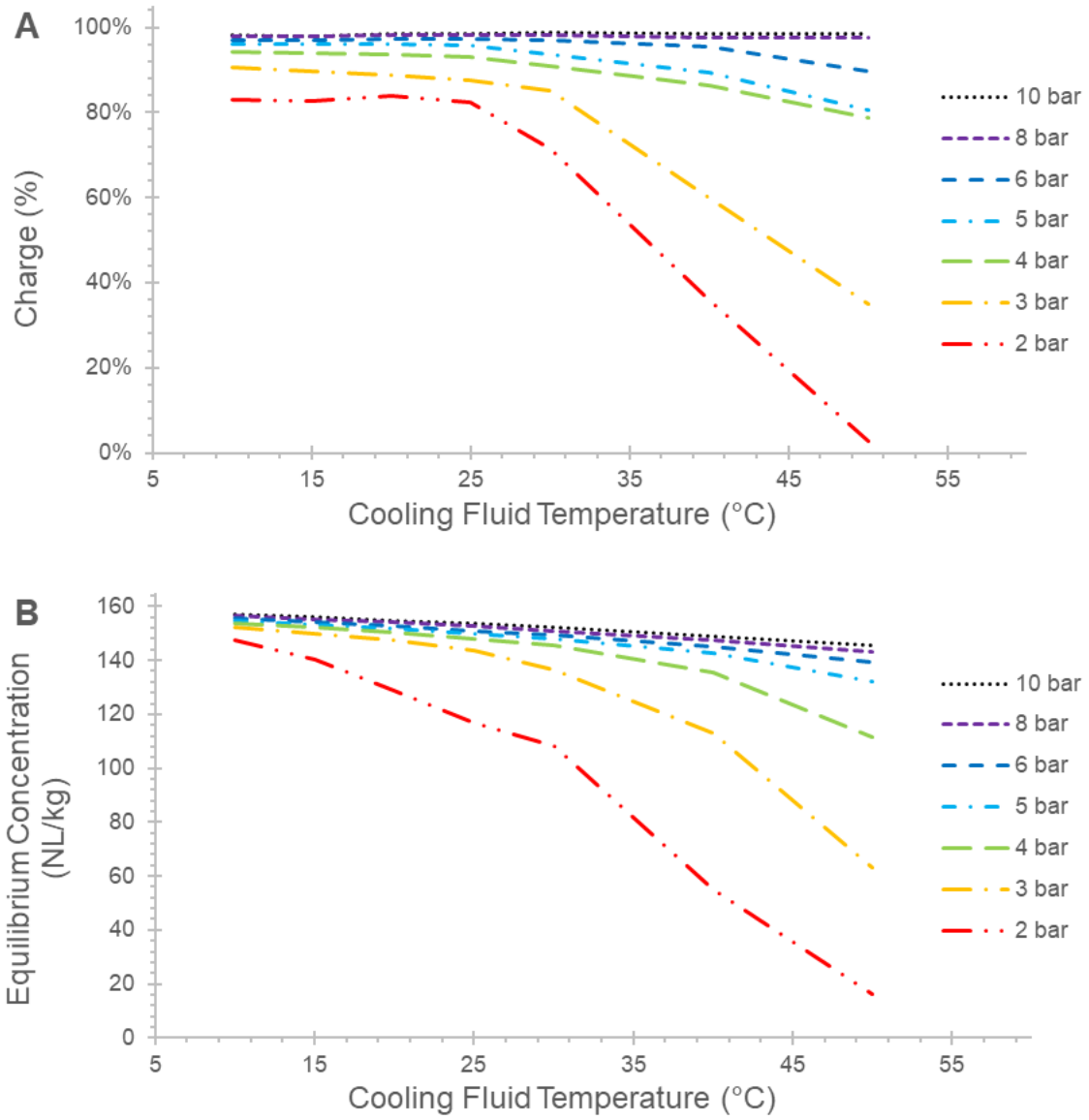

Figure 8. Absorption sensitivity analysis with (A) final charge percentage after 90 min as a function of feed gas pressure and cooling fluid temperature, and (B) the equilibrium absorption concentration as a function of feed gas pressure and cooling fluid temperature.

Regarding Figure 9A, at lower heating fluid temperatures, little to no absorption takes place aside from the lowest required discharge gas pressure of 8 bar. Furthermore, at heating fluid temperatures between 90 °C and 120 °C, more absorption takes place, with the required discharge gas pressure determining the rate of discharge. It should be noted that in the range of 100 °C to 110 °C, the heating fluid temperature curves almost form a temporary plateau of sorts. Then, at heating fluid temperatures beyond 120 °C, another plateau forms in terms of heating fluid temperature, and only the required discharge gas pressure determines the rate of desorption.

Thus, considering Figure 9A would suggest that there is a minimum heating fluid temperature requirement for desorption to take place on any meaningful scale. Similarly, the required discharge gas pressure is a key determining factor that negatively affects how much hydrogen will be able to be discharged at that pressure.

While higher heating fluid temperatures counteract this negative effect of required discharge gas pressure on the rate and amount of discharge, there is still an inherent limit to the pressure the metal hydride can generate during discharge. This is apparent when 18 bar is discharged considerably less than 16 bar at the heating fluid temperatures exceeding 120 °C.

This is similar to what is hypothesised when considering Equation 9 and the isotherms represented in Figure 3. More so when considering Figure 9B, which has a similar inverse trend to Figure 9A, suggesting a relationship between the equilibrium desorption concentration and the discharge amount as well as the discharge rate.

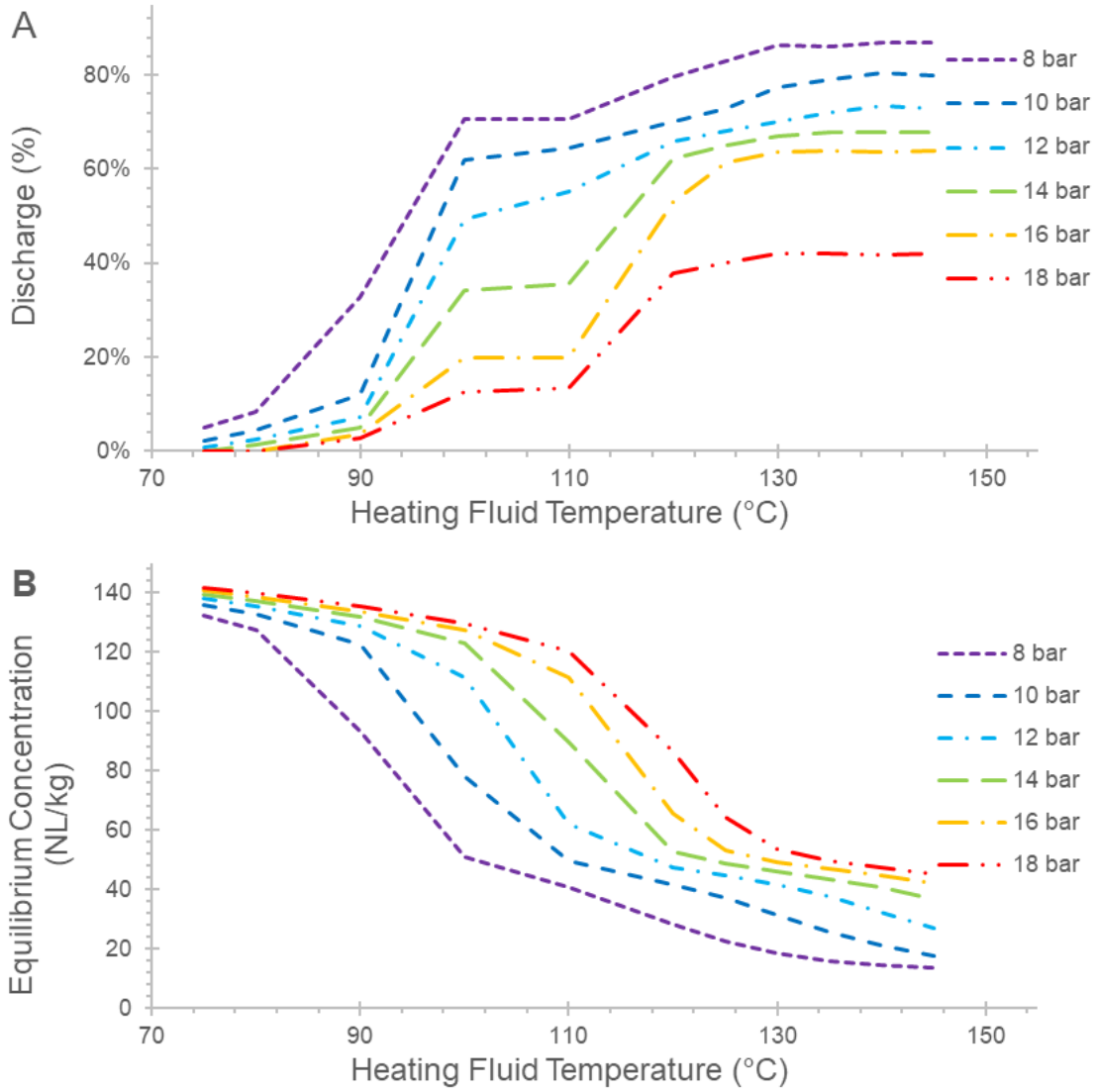

Figure 9. Desorption sensitivity analysis with (A) discharge percentage after 80 min as a function of required discharge gas pressure and heating fluid temperature, and (B) the equilibrium desorption concentration as a function of required discharge gas pressure and heating fluid temperature.

6. Conclusion

The sensitivity analysis shows that for this particular reactor, the respective equilibrium concentrations of hydrogen in the metal hydride complex have a strong predictive factor for the rate and amount of both hydrogen charge and discharge. These equilibrium concentrations are determined by the equilibrium temperature and the equilibrium pressure of the system per the pressure-concentration-temperature isotherms. Per the thermodynamic laws, the equilibrium temperature is determined by the temperature of the cooling and heating fluid, depending on the state of

operation. Similarly, equilibrium pressure is determined by the pressure of the feed gas during the charge state or what the pressure regulator was set at during the discharge state. Therefore, Figure 8 proves that the reactor operation is sensitive to feed gas pressure and cooling fluid temperature during absorption. Similarly, Figure 9 proves that the reactor operation is sensitive to the required discharge gas pressure and heating fluid temperature during desorption.

From the sensitivity analysis, the following core conclusions can be made regarding the operation of this specific metal hydride reactor.
For charging, while considering a charging time of 90 minutes:

i. The temperature of the cooling fluid has a negligible effect under 25 °C.
ii. Feed gas pressure has a negligible effect if the cooling fluid temperature remains under 25 °C.
iii. The temperature of the cooling fluid has an amplified effect beyond 25 °C.
iv. The Feed gas pressure has a reduced effect above 4 bar.
v. Under a feed gas pressure of 4 bar, performance is significantly reduced under a cooling fluid temperature of 25 °C.
vi. As such, ideally, the cooling fluid temperature should remain under 25 °C to save cost from precompression of the hydrogen.
vii. In hot climates, the higher cooling fluid temperatures can be counteracted by precompression of the hydrogen to 4 bar for the feed hydrogen.

For discharging, while considering a discharge time of 80 minutes, which would be the operation time at full capacity:

i. Above a heating fluid temperature of 115 °C, the heating fluid temperature has a negligible effect.
ii. Below a heating fluid temperature of 90 °C, the unit does not discharge any significant amount of hydrogen.
iii. The effect of heating fluid temperature between 90 °C and 115 °C is amplified.
iv. Required discharge pressure above 16 bar significantly reduces the amount of hydrogen discharged.
v. Between 90 °C and 115 °C heating fluid temperature, the required gas pressure has an amplified effect.
vi. Ideally, the heating fluid temperature should be around 115 °C to save on heating costs.
vii. The required gas pressure on the pressure regulator during discharge should not be set higher than 16 bar for the discharge of hydrogen.

Acknowledgements

Faurie DG would like to acknowledge the Tshwane University of Technology, specifically the Department of Research and Innovation, for the financial assistance and resources provided. Finally, HySA-Systems of the University of Western Cape is acknowledged for the experimental data used to validate the model.

References

Abdechafik, E. harrak, Ait Ousaleh, H., Mehmood, S., Filali Baba, Y., Bürger, I., Linder, M. & Faik, A. An analytical review of recent advancements on solid-state hydrogen storage. International Journal of Hydrogen Energy. 52:1182–1193. 2024. DOI: 10.1016/J.IJHYDENE.2023.10.218.

Akanji, O. & Kolesnikov, A. V. Modelling of Hydrogen Adsorption/Desorption in Metal Hydride Reactor. Journal of Computational and Theoretical Nanoscience. 7(10):2112–2115. 2010. DOI: 10.1166/jctn.2010.1592.

Aziz, M. Liquid Hydrogen: A Review on Liquefaction, Storage, Transportation, and Safety. Energies. 14(18):5917. 2021. DOI: 10.3390/en14185917.

Baldissin, D. & Lombardo, D. Thermofluidynamic Modelling of Hydrogen Absorption and Desorption in a LaNi4.8Al0.2 Hydride Bed. In Proceedings of the COMSOL Conference. Milan. 1–7. 2009.

Bellosta von Colbe, J., Ares, J.-R., Barale, J., Baricco, M., Buckley, C., Capurso, G., Gallandat, N., Grant, D.M., et al. Application of hydrides in hydrogen storage and compression: Achievements, outlook and perspectives. International Journal of Hydrogen Energy. 44(15):7780–7808. 2019. DOI: 10.1016/j.ijhydene.2019.01.104.

Busqué, R., Torres, R., Husar, A. & Torres, R. Numerical modeling and experimental analysis of the desorption process in a metal hydride hydrogen storage system. University in Barcelona. 2017 Available: http://digital.csic.es/bitstream/10261/168974/1/numerisystem.pdf.

Cavo, M., Rivarolo, M., Gini, L. & Magistri, L. An advanced control method for fuel cells - Metal hydrides thermal management on the first Italian hydrogen propulsion ship. International Journal of Hydrogen Energy. 2023. 48(54):20923–20934. DOI: 10.1016/J.IJHYDENE.2022.07.223.

Churchard, A.J., Banach, E., Borgschulte, A., Caputo, R., Chen, J.-C., Clary, D., Fijalkowski, K.J., Geerlings, H., et al. A multifaceted approach to hydrogen storage. Physical Chemistry Chemical Physics. 13(38):16955. 2011. DOI: 10.1039/c1cp22312g.

Dehouche, Z., Grimard, N., Laurencelle, F., Goyette, J. & Bose, T.K. Hydride alloys properties investigations for hydrogen sorption compressor. Journal of Alloys and Compounds. 399(1–2):224–236. 2005. DOI: 10.1016/j.jallcom.2005.01.029.

Dong, Z., Wang, Y., Wu, H., Zhang, X., Sun, Y., Li, Y., Chang, J., He, Z., et al. A design methodology of large-scale metal hydride reactor based on schematization for hydrogen storage. Journal of Energy Storage. 2022. 49:104047. DOI: 10.1016/j.est.2022.104047.

Drawer, C., Lange, J. & Kaltschmitt, M. Metal hydrides for hydrogen storage – Identification and evaluation of stationary and transportation applications. Journal of Energy Storage. 2024. 77:109988. DOI: 10.1016/J.EST.2023.109988.

Faurie, D.G. & Premlall, K. Simulating non-ideal AB5 metal hydride pressure–concentration–temperature isotherms in MATLAB. Multiscale and Multidisciplinary Modeling, Experiments and Design. 8(3):194. 2025. DOI: 10.1007/s41939-025-00780-9.

Ghritalahre, B., Bhargav, V.K., Gangil, S., Sahu, P. & Sahu, R.K. Next generation bio-derived 3D-hierarchical porous material for remarkable hydrogen storage – A brief critical review. Journal of Power Sources. 2023. 587:233648. DOI: 10.1016/J.JPOWSOUR.2023.233648.

Handique, A.J., Peer, R., Haas, J., Osorio-Aravena, J.C. & Reyes-Chamorro, L. Distributed hydrogen systems: A literature review. International Journal of Hydrogen Energy. 85:427–439. 2024. DOI: 10.1016/J.IJHYDENE.2024.08.206.

Hydrogen and Fuel Cell Technologies Office. H2@Scale. 2020. Available: https://www.energy.gov/eere/fuelcells/h2scale [2020, October 24].

Jeje, S.O., Marazani, T., Obiko, J.O. & Shongwe, M.B. Advancing the hydrogen production economy: A comprehensive review of technologies, sustainability, and future prospects. International Journal of Hydrogen Energy. 2024. 78:642–661. DOI: 10.1016/J.IJHYDENE.2024.06.344.

Jemni, A., Nasrallah, S. Ben & Lamloumi, J. Experimental and theoretical study of a metal-hydrogen reactor. International Journal of Hydrogen Energy. 24:631–644. 1999.

Li, H., Cao, X., Liu, Y., Shao, Y., Nan, Z., Teng, L., Peng, W. & Bian, J. Safety of hydrogen storage and transportation: An overview on mechanisms, techniques, and challenges. Energy Reports. 8:6258–6269. 2022. DOI: 10.1016/J.EGYR.2022.04.067.

Li, X., Yuan, Z., Liu, C., Sui, Y., Zhai, T., Hou, Z., Han, Z. & Zhang, Y. Research progress in improved hydrogen storage properties of Mg-based alloys with metal-based materials and light metals. International Journal of Hydrogen Energy. 50:1401–1417. 2024. DOI: 10.1016/J.IJHYDENE.2023.09.265.

Lototskyy, M. V. New model of phase equilibria in metal - Hydrogen systems: Features and software. International Journal of Hydrogen Energy. 41(4):2739–2761. 2016. DOI: 10.1016/j.ijhydene.2015.12.055.

Lototskyy, M., Klochko, Y., Wafeeq Davids, M., Pickering, L., Swanepoel, D., Louw, G., van der Westhuizen, B., Chidziva, S., et al. Industrial-scale metal hydride hydrogen compressors developed at the South African Institute for Advanced Materials Chemistry. Materials Today: Proceedings. 5(4):10514–10523. 2018. DOI: 10.1016/j.matpr.2017.12.383.

Lototskyy, M. V., Tolj, I., Pickering, L., Sita, C., Barbir, F. & Yartys, V. The use of metal hydrides in fuel cell applications. Progress in Natural Science: Materials International. 27(1):3–20. 2017 DOI: 10.1016/j.pnsc.2017.01.008.

Mellouli, S., Askri, F., Dhaou, H., Jemni, A. & Ben Nasrallah, S. Numerical study of heat exchanger effects on charge/discharge times of metal–hydrogen storage vessel. International Journal of Hydrogen Energy. 34(7):3005–3017. 2009. DOI: 10.1016/j.ijhydene.2008.12.099.

Pasini, J.M., Corgnale, C., Van Hassel, B.A., Motyka, T., Kumar, S. & Simmons, K.L. Metal hydride material requirements for automotive hydrogen storage systems. International Journal of Hydrogen Energy. 38(23):9755–9765. 2013. DOI: 10.1016/j.ijhydene.2012.08.112.

Prachi, P., Wagh, M.M. & Aneesh, G. A Review on Solid State Hydrogen Storage Material. Advances in Energy and Power. 4(2):11–22. 2016. DOI: 10.13189/aep.2016.040202.

Qureshi, F., Yusuf, M., Ahmed, S., Haq, M., Alraih, A.M., Hidouri, T., Kamyab, H., Vo, D.V.N., et al. Advancements in sorption-based materials for hydrogen storage and utilization: A comprehensive review. Energy. 309:132855. 2024. DOI: 10.1016/J.ENERGY.2024.132855.

Salman, M.S., Lai, Q., Luo, X., Pratthana, C., Rambhujun, N., Costalin, M., Wang, T., Sapkota, P., et al. The power of multifunctional metal hydrides: A key enabler beyond hydrogen storage. Journal of Alloys and Compounds. 920:165936. 2022. DOI: 10.1016/j.jallcom.2022.165936.

Song, C., Klebanoff, L.E., Johnson, T.A., Chao, B.S., Socha, A.F., Oros, J.M., Radley, C.J., Wingert, S., et al. Using metal hydride H2 storage in mobile fuel cell equipment: Design and predicted performance of a metal hydride fuel cell mobile light. International Journal of Hydrogen Energy. 39(27):14896–14911. 2014. DOI: 10.1016/j.ijhydene.2014.07.069.

Tarasov, B.P., Bocharnikov, M.S., Yanenko, Y.B., Fursikov, P. V, Minko, K.B. & Lototskyy, M. V. Metal hydride hydrogen compressors for energy storage systems: layout features and results of long-term tests. Journal of Physics: Energy. 2(2):024005. 2020. DOI: 10.1088/2515-7655/ab6465.

Wang, D., Wang, Y., Huang, Z., Yang, F., Wu, Z., Zheng, L., Wu, L. & Zhang, Z. Design optimization and sensitivity analysis of the radiation mini-channel metal hydride reactor. Energy. 173:443–456. 2019. DOI: 10.1016/J.ENERGY.2019.02.033.

Yartys, V.A. & Lototsky, M. V. An Overview of Hydrogen Storage Methods. In Hydrogen Materials Science and Chemistry of Metal Hydrides. V. 172. 75–104. 2004. DOI: 10.1007/1-4020-2669-2_7.

Biographies

Douw Gerbrand Faurie is a Doctor of Engineering candidate in the discipline of Chemical Engineering from the Tshwane University of Technology scheduled to graduate in 2025. He graduated Master of Engineering in Chemical Engineering Cum Laude in 2022, with his research focusing on improving the designing practices and the knowledge base regarding metal hydride-based hydrogen storage tanks using computational fluid dynamics. Currently, Douw serves as a machine learning expert on multiple projects with his doctoral research focusing on creating a digital twin of a metal hydride reactor to be used for solid-phase hydrogen storage applications.

Dr Kasturie Premlall is a permanently appointed Researcher and Lecturer in the Department of Chemical, Metallurgical and Materials Engineering, Faculty of Engineering and the Built Environment at Tshwane University of Technology, Pretoria, South Africa. She has previously held the position of the Section Head for Chemical Engineering. She has completed a Master's degree in corrosion inhibition studies in the degradation of reinforcement steel material in structural material, focusing on the reinforcement of concrete structures and ion metal ingress. She earned her Ph.D. in Chemical Engineering from the University of Witwatersrand, South Africa. Her focused research interests include carbon capture and sequestration (CCS), corrosion technology focusing on green corrosion inhibitors, hydrogen storage and metal-organic frameworks (MOFs) for carbon dioxide (CO2) capture; landfill biogas recovery (process and materials) for methane (CH4) capture and the recovery, and interest in rare earth elements (REEs) from AMD and coal fly ash in South Africa.

Prof Andrei Kolesnikov graduated from the Moscow Institute of Chemical Engineering in 1979. He obtained PhD degree from the same institution in 1985. The topic of his PhD work was entitled "Multi-jet plasma chemical reactor for aluminium oxide nanopowder production". He worked as an applied researcher in the State Laboratory of Plasma Processes at Almaty Power Engineering Institute from 1979 to 1992. He continued his research work in South Africa, where he worked at the Nuclear Energy Corporation of South Africa from 1992 to 1999, and at Tshwane University of Technology from 1999 up to 2022. His research interests include the modelling of multi-phase high-temperature processes, plasma technologies, complex systems agent-based modelling, process control and optimisation.

Dr Mykhaylo Lototskyy graduated from the Moscow State University in 1977 and received his PhD degree in 1992 from the Lviv State University (Ukraine). He held postdoctoral positions at the Institute for Energy Technology (Norway, 2002–2003) and the University of the Western Cape. Currently, Dr Lototskyy is a Senior Researcher at the South African Institute for Advanced Materials Chemistry and a Key Technology Specialist on Hydrogen Storage and Related Applications within the South African Hydrogen and Fuel Cell Technologies RDI Program (HySA Systems Competence Centre hosted by UWC). Dr Lototskyy is an internationally recognised and renowned researcher in the fields of Hydrogen Energy and Technology, hydrogen storage, material science and applications of metal hydrides.